Tellus (2005), 57B, 40–50
Printed in UK. All rights reserved

TELLUS

Overview of aerosol microphysics at Arctic sunrise: measurements during the NICE renoxification study

By S. NYEKI[1,2,*], G. COULSON[1], I. COLBECK[1], K. ELEFTHERIADIS[3], U. BALTENSPERGER[2] and H. J. BEINE[4], [1]*Institute for Environmental Research, University of Essex, Colchester, Essex CO4 3SQ, UK;* [2]*Laboratory of Atmospheric Chemistry, Paul Scherrer Institut, CH-5232 Villigen-PSI, Switzerland;* [3]*Environmental Radioactivity Lab., NCSR Demokritos, 15310 Ag. Paraskevi, Attiki, Athens, Greece;* [4]*CNR-IIA, Via Salaria Km 29.3, I-00016 Monterotondo Scalo (Roma), Italy*

(Manuscript received 24 February 2004; in final form 11 May 2004)

ABSTRACT

Extensive aerosol and trace gas measurements were conducted at Ny-Ålesund (Svalbard) before and after Arctic sunrise in 2001 (NICE Dark and Light intensive campaigns) in order to study the possible role of aerosols in the renoxification mechanism. This study reports aerosol physical measurements over a continuous 3-month period. Arctic and sub-Arctic air masses dominated the measurement period and were characterized by low number ($N \sim 275$ and 590 cm^{-3} respectively) and surface area ($S \sim 39$ and 28 μm^2 cm^{-3}) concentrations (measured range $d = 14$–740 nm) except for two Arctic haze events with high concentrations in springtime ($N \sim 1140$ cm^{-3} and ~ 125 μm^2 cm^{-3}). Excluding these events, aerosol volatility measurements indicated no significant variation in the volatile (∼0.40), semi-volatile (∼0.32) or refractory (∼0.28) volume fractions which are commonly attributed to H_2SO_4, $(NH_4)_2SO_4/NH_4HSO_4$ and soot/dust/sea-salt aerosol.

1. Introduction

Recent studies during polar sunrise in the Arctic and Antarctic have not only observed enhanced NO_x (NO_2 + NO) concentrations but also a diurnal cycle in NO_2 (e.g. Honrath et al., 2000; Dibb et al., 2002). So-called renoxification (i.e. reduction) of NO_3^- within or on the snow surface to NO_x and HONO as a result of photochemistry is considered to be the dominant mechanism. However, there is some limited evidence to suggest that aerosols may play a role (Hauglustaine et al., 1996; Aumont et al., 1999), despite current understanding that various snow/ice surfaces (e.g. frost flowers, wind-blown fragments, cirrus ice particles) are most probably responsible for renoxification (e.g. Honrath et al., 2000; Dibb et al., 2002). While most renoxification field studies have used sophisticated measurement techniques many have only been conducted over short time periods under optimum weather conditions. In addition, ambient aerosol properties with respect to renoxification have largely remained uncharacterized.

The EC project "The Nitrogen Cycle and Effects on the Oxidation of Atmospheric Trace Species at High Latitudes" (NICE) was concerned with the source and the mechanism of NO_x release. Extensive trace gas, aerosol, snow and meteorological measurements were conducted at the Ny-Ålesund Arctic baseline station (sea level, 78.90°N, 11.88°E, Svalbard) during a 3-month period from Arctic winter to spring 2001 (Beine et al., 2003). The aim was to further elucidate the renoxification process, as well as to assess the possible role of aerosols. Measurements are complemented by two previous Large-Scale Facility (LSF; European Union project) campaigns conducted at the Zeppelin station (474 m above sea level) near Ny-Ålesund (sea level), Svalbard, in late summer 1998 (LSF I: August–September) and spring 1999 (LSF II: April–May). Ny-Ålesund and the Zeppelin site are part of the Global Atmosphere Watch (GAW) network and are categorized as an Arctic baseline station due to their remote location. The present study gives an overview of on-line aerosol microphysical measurements during Arctic sunrise and late summer. Trace gas concentrations from annular denuders have been discussed by Beine et al. (2003), while future work (G. Coulson et al., in preparation) will discuss renoxification with respect to aerosols and trace gases.

2. Instrumentation and methods

NICE intensive field campaigns were conducted during Arctic sunrise from 21 February to 8 March 2001 (day of year (DOY) = 52–67; winter/twilight) and 24 April to 19 May 2001 (DOY = 114–139; Arctic spring), hereafter referred to as the Dark

*Corresponding author.
e-mail: stephan.nyeki@psi.ch

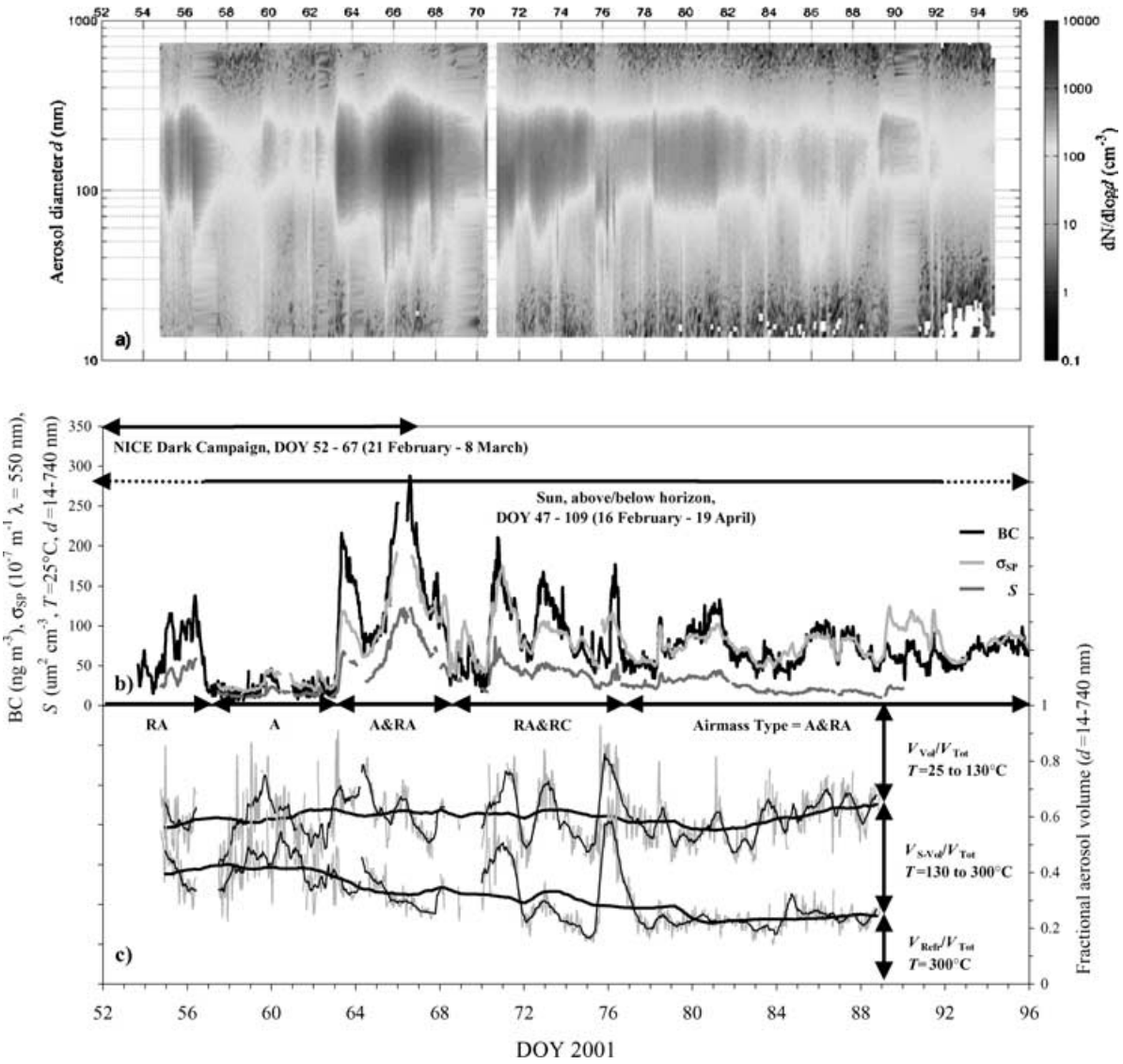

Fig 1. Aerosol time-series during the Dark intensive of: (a) number size spectra $\mathrm{d}N/\mathrm{d}\log d$, (b) aerosol black carbon (BC), scattering coefficient σ_{SP} and surface area concentration S (all 1 h resolution) and (c) the fractional aerosol volume for the volatile (V_{Vol}/V_{Tot}), semi-volatile ($V_{S\text{-}Vol}/V_{Tot}$) and (V_{Refr}/V_{Tot}) refractory fractions (all 1 h resolution, grey line; 12 h running mean, black line; 7 d running mean, heavy black line). Horizontal bars indicate the air mass origin from 5 d back-trajectory analysis: A = Arctic, N = North Atlantic, RA = Russian Arctic region, RC/S = Central Russia/Siberia, W = West Europe. Note that BC concentrations are based on the manufacturer's calibration (see text for further details).

and Light intensives, respectively. Arctic night-time ended on 16 February (DOY 47; i.e. the first Arctic sunrise), and the sun was above the horizon for 24 h as of 19 April (DOY 109). These periods are graphically represented in Figs 1 and 2 and are further described in Section 3. Measurements were continued between intensives allowing a 3-month dataset to be collected. Gas gradient measurements at two heights above ground level were the basis of the NICE project (Beine et al., 2001a, 2003). As ambient aerosols are distributed inhomogeneously in the atmosphere, even in the absence of fluxes or over several metres distance, it was decided to conduct aerosol measurements at a single height with as high a temporal resolution as possible. An overview of the Dark and Light intensives is described by Beine et al. (2003) and a site map is presented by Teinilä et al. (2003). A more detailed description of instrumentation and methods relevant to this work is given below.

An undisturbed, snow-covered area during the winter/spring period was a necessary pre-requisite for studying the renoxification process, for which the Amundsen mast site (sea level), about 300 m southeast of Ny-Ålesund, was chosen. The location also ensured that the predominant southeasterlies, blowing over inland glacier sheets, kept local pollution to a minimum.

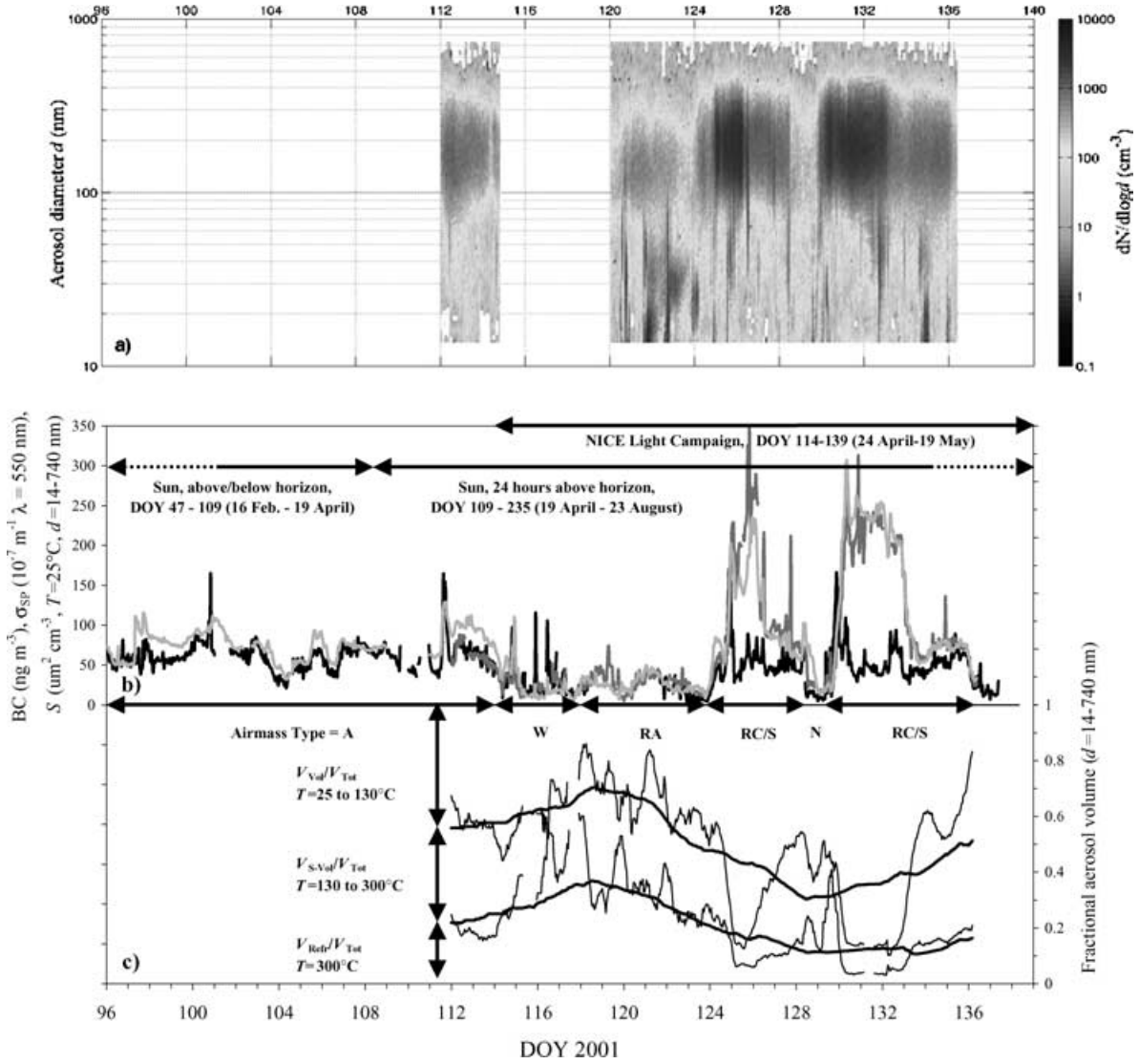

Fig 2. Aerosol time-series during the Light intensive, otherwise the same as for Fig. 1. Curves for the fractional volume (lower panel) with a 1 h resolution have been omitted for clarity. Note that the *y*-axis scales are the same as in Fig. 1.

A large restricted region was established around the measurement site in order to keep the snow surface as pristine as possible. The NICE site was about 20 m from the shore of the Kongsfjorden Fjord (20 km long, 4–10 km wide) which is normally frozen until May/June but was not the case in 2001. Most of the fjord apart from a small part close to the calving glacier remained open throughout the winter and spring, which is exceptional (Svendsen et al., 2002). The prevailing southeasterlies thus flowed parallel to the fjord for about 11 km before reaching the NICE measurement site. The extent to which the open waters affected sampled air masses is unknown but sea-salt concentrations may have been elevated. Instruments used in this study were housed in a cabin and sampled from a common snow-hood inlet (2.5 m above ground level), placed on the container roof, with a 1 m steel tube (3 cm diameter) delivering sample air to instruments. As losses due to sedimentation and diffusion were estimated at <4% due to the high flow rate (>70 l min^{-1}) in the inlet line, corrections were not made. Heating of the incoming air to below the relative humidity (RH) at which aerosols begin to grow (RH = 40–50%) was unnecessary due to an indoor cabin temperature of ∼25 °C and hence low RH (<10%). Aerosol number size distributions (d = 14–740 nm; 5 min resolution) were measured with a scanning mobility particle sizer (SMPS, TSI 3934) consisting of a TSI 3071 differential mobility analyser (DMA) and TSI 3010 condensation particle counter (CPC). Spectra were used to determine the aerosol number (N), surface area (S) and volume (V) concentrations over this size range. The SMPS measures the mobility equivalent diameter which is inverted to a spherical equivalent particle diameter. If renoxification occurs on aerosol surfaces as well as on ice/snow

surfaces then a correlation between NO_x and S concentrations may be expected. Qualitative information on the aerosol chemical composition may be obtained by pre-conditioning the aerosol sample in a heated volatility tube or so-called thermodenuder (e.g. Burtscher et al., 2001, and references therein). Volatility SMPS (VSMPS) spectra were measured at $T = 25$ (i.e. ambient cabin), 130 and 300 °C. The range $T = 25$–130 °C is commonly attributed to H_2SO_4 (defined here as volatile aerosol), $T = 130$–300 °C to sulfate and bisulfate (semi-volatile) and the remaining aerosol at $T = 300$ °C is known as refractory aerosol (elemental carbon, sea-salt and mineral dust) (e.g. Smith and O'Dowd, 1996). These channels were used to calculate S and V for the total, volatile, semi-volatile and refractory aerosols: V_{Tot}, V_{Vol}, $V_{\mathrm{S\text{-}Vol}}$ and V_{Refr}. Care must be taken in interpreting volatility results as organic compounds (OC) may contribute significantly to the total aerosol volume but have a wide range of vapour pressures and hence do not generally exhibit specific thermal characteristics. A positive artefact may thus result as a range of OC compounds have been observed in the Arctic (Cecinato et al., 2000; Narukawa et al., 2002, and references therein).

The thermodenuder was constructed of a heated, coiled copper-tube (length 100 cm, 4.5 mm inner diameter) wrapped in a thermostatically controlled heating tape. The 1.0 l min^{-1} flow rate through the thermodenuder (i.e. determined by the CPC flow rate) ensured a sufficiently long residence time (4 s) for volatile species to be removed to the thermodenuder wall. An effective time resolution of 60 min per temperature was attained, as the single, available thermodenuder took about 35 min to cool down from 300 to 25 °C using a cooling fan. A closed-loop pump arrangement was used for the SMPS sheath and excess flows, which were regulated using a critical orifice calibrated at 3.1 l min^{-1}. Apart from the stability of this configuration, the same gas composition was ensured both inside the DMA and in the sampled air, thereby minimizing any possible sampling artefacts. Flows were regularly calibrated with a bubble flow meter and precision was found to be ±2%. VSMPS spectra were corrected for losses due to thermophoresis and diffusion according to laboratory experiments (Burtscher et al., 2001). Corrections were typically +10% and rose to +30% for $d < 20$ nm at $T = 300$ °C. All measurements reported here have been corrected to STP conditions (273.15 K and 1013 mbar).

The aerosol total scattering coefficient (σ_{SP}) was measured with a three-wavelength integrating nephelometer (TSI model 3563; $\lambda = 450$, 550 and 700 nm). As σ_{SP} exhibits a dependency on d^2 over the accumulation mode size range ~ 100–1000 nm, it is a good proxy for S. Data were collected with a 5 min resolution and used to construct hourly averages, for which a detection limit σ_{SP} (550 nm) $\sim 1.3 \times 10^{-7}$ m^{-1} was determined. The aerosol black carbon (BC) concentration was determined using an AE-31 aethalometer (Magee Scientific) with a measured 1 h detection limit of 1.5 ng m^{-3}. Measurements are nominally based on the manufacturer's calibration where the specific absorption coefficient $\alpha_{\mathrm{AP}} = 16.6$ m^2 g^{-1} at $\lambda = 880$ nm. A calibrated value $\alpha_{\mathrm{AP}} \sim 12.1$ m^2 g^{-1} using an AE-9 aethalometer and EC thermal method was determined during the LSF I campaign. However, the manufacturer's calibration is used in the present study until a calibration based on the present data set is available, and it should therefore be noted that the reported BC concentrations could be too low by a factor of ~1.4. However, a possible correction of this magnitude would not alter the conclusions regarding BC presented here.

In-cloud periods were detected using a Gerber cloud monitor (particulate volume monitor—PVM-100, Gerber Scientific) to measure the liquid water content. As such periods were rare during the measurement period, these data were removed from the data set so that only out-of-cloud periods are reported here. Meteorological data for Ny-Ålesund were available at our measurement site (Beine et al., 2003) and from the Alfred Wegener Institute (AWI). In summary, daily average temperatures varied from $T = -13$ °C in February to -5 °C in May 2001, average relative humidity (RH) was 60–80%, and average wind speed was <4 m s^{-1}. Air mass back-trajectory analyses were provided by the NOAA HYSPLIT model (Draxler and Hess, 1998). The origin of 5 d air mass back-trajectories are classified in a similar manner to Beine et al. (1996). Definitions include: (1) the Arctic region (A; north of 80°N and the whole of Greenland), (2) Western Europe (W; the sector from West Ireland to the Urals), (3) Central Russia/Siberia (RC/S; east of the Urals), (4) the Russian Arctic (RA; east of the Urals, north of the Russian coast and south of 80°N) and (5) the North Atlantic (N; west of Ireland and south of 80°N). These definitions are based on air masses spending at least 4 days over the region of origin before arrival at Ny-Ålesund.

3. Results and discussion

3.1. Aerosol properties: time-series

Approximately 1300 size spectra were collected at each thermodenuder temperature during the February to May 2001 period, which included the Dark and Light intensives. A detailed analysis using N and BC concentrations was used to remove obvious local pollution events from the database. Figures 1 and 2 illustrate time-series of various parameters measured during both intensives, respectively, and include: (a) aerosol number spectra $\mathrm{d}N/\mathrm{d}\log d$, (b) BC, σ_{SP} ($\lambda = 550$ nm) and S, and (c) $V_{\mathrm{Vol}}/V_{\mathrm{Tot}}$, $V_{\mathrm{S\text{-}Vol}}/V_{\mathrm{Tot}}$ and $V_{\mathrm{Refr}}/V_{\mathrm{Tot}}$. As the origin and type of air mass has a fundamental effect on aerosol properties (Nilsson and Barr, 2001) these are also illustrated in both figures. Air masses from February to May 2001 mainly originated from the Arctic, the Russian Arctic and Central Russia/Siberia. In general, aerosol concentrations were higher during the Dark than the Light intensive if two Arctic haze events during the latter intensive are excluded (see Table 1 for statistical parameters).

Table 1. Average (Avg.), standard deviation (SD) and median (Med.) aerosol statistical parameters during the Dark and Light intensives (see text for definition of air mass types). Results according to air mass origin are only reported for durations >1–2 d. All results are corrected to STP conditions.

		Dark intensive 21 Feb.–8 Mar. 2002 (DOY = 52–67)			Light intensive 24 April–19 May 2002 (DOY114–139)		
Aerosol parameter		Whole period (DOY 52–67)	Air mass A (DOY 57.0–63.0)	Air mass RC/S&W (DOY 63.0–68.4)	Whole period (DOY 114–139)	Air mass RA (DOY 117.9–123.9)	Air mass RA/S (DOY 123.9–128.5, 129.3–136.1)
N conc.[a]	Avg.	275	117	498	860	588	1137
(cm^{-3})	SD	224	25	195	1554	452	2064
	Med.	162	115	461	565	464	654
S conc.[a]	Avg.	39	15	69	80	28	125
($\mu m^2\ cm^{-3}$)	SD	32	4	29	74	12	76
	Med.	25	14	65	50	28	90
σ_{SP} (m^{-1})	Avg.	5.76×10^{-6}	2.67×10^{-6}	1.11×10^{-5}	7.80×10^{-6}	2.57×10^{-6}	1.27×10^{-5}
$\lambda = 550$ nm	SD	4.68×10^{-6}	7.94×10^{-7}	3.83×10^{-6}	7.35×10^{-6}	9.22×10^{-7}	7.44×10^{-6}
	Med.	3.55×10^{-6}	2.33×10^{-6}	1.11×10^{-5}	5.42×10^{-6}	2.39×10^{-6}	8.73×10^{-6}
BC conc.[b]	Avg.	72	22	142	41	18	54
($ng\ m^{-3}$)	SD	65	9	56	26	9	23
	Med.	42	19	136	39	19	48
V_{Vol}/V_{Tot}	Avg.	0.39	0.42	0.37	0.50	0.32	0.62
	SD	0.07	0.07	0.06	0.20	0.09	0.18
	Med.	0.39	0.42	0.36	0.46	0.33	0.58
V_{S-Vol}/V_{Tot}	Avg.	0.22	0.16	0.31	0.27	0.34	0.25
	SD	0.09	0.06	0.05	0.19	0.12	0.09
	Med.	0.23	0.15	0.31	0.33	0.34	0.30
V_{Refr}/V_{Tot}	Avg.	0.39	0.42	0.33	0.22	0.34	0.13
	SD	0.06	0.05	0.05	0.14	0.10	0.08
	Med.	0.38	0.43	0.33	0.21	0.33	0.12

[a]For the range $d = 14$–740 nm.

[b]Using manufacturer's calibration, see text.

Significant variability in aerosol concentrations was attributed to air mass changes. A more detailed description of Figs 1a,b and 2a,b now follows.

The Dark intensive was generally characterized by either relatively low or high aerosol concentrations. A clean period occurred from DOY 57.0–63.0 when air masses from the Arctic (labelled "A" in Fig. 1) were responsible for amongst the lowest aerosol concentrations during NICE (averages $N = 117\ cm^{-3}$, $S = 15\ \mu m^2\ cm^{-3}$, BC = 22 $ng\ m^{-3}$). However, aerosol concentrations increased by almost a factor 5 in the subsequent period from DOY 63.0–68.4 when air masses also came from the Arctic but made landfall with the Russian Arctic according to the trajectory analysis (labelled "A& RA" in Fig. 1). Correlation coefficients between N, BC, S and σ_{SP} were in the range $R =$ 0.80–0.97 during air mass A& RA and $R = 0.41$–0.84 during air mass A. The stark contrast in these two periods, despite their similar air mass characteristics, was most likely due to aerosol removal by wet scavenging at some stage in the air mass history.

Measurements during the Light intensive illustrate a greater variability in all parameters. Russian Arctic air masses towards the beginning of the Light intensive resulted in relatively low aerosol concentrations ($N = 588\ cm^{-3}$; see Table 1 for other parameters). However, two large Arctic haze events from DOY 123.9–128.5 and 129.3–136.1 then dominated the remainder of the Light intensive, when significant increases in N, S and σ_{SP} (averages: 1137 cm^{-3}, 125 $\mu m^2\ cm^{-3}$, $1.27 \times 10^{-5}\ m^{-1}$ respectively) but not in BC (54 $ng\ m^{-3}$) were observed. Trajectory analyses indicated that both air masses originated from Central Russia/Siberia and were mainly transported close to the surface layer. These air masses were briefly interrupted by a clean air mass from the North Atlantic as observed by the highest Na^+ concentrations ($\sim$3.0 $\mu g\ m^{-3}$) measured during NICE (unpublished data). Correlation coefficients during both haze events between BC, S and σ_{SP} were in the range $R = 0.41$–0.60 during the Light intensive when excluding these events. During the haze events, S and σ_{SP} exhibited $R = 0.92$, but only $R \sim 0.15$ with BC. These haze events will be discussed later in greater detail.

Most previous aerosol measurements at Ny-Ålesund were conducted during the Arctic spring (e.g. Covert and

Table 2. Previous aerosol measurements at Ny-Ålesund and those from the present study. See text for explanation of measured parameters.

	Aerosol parameter				
	N conc. (cm^{-3})	S conc. ($\mu m^2\ cm^{-3}$)	σ_{SP} (m^{-1}) $\lambda = 550$ nm	BC conc. ($ng\ m^{-3}$)	V_{Vol}/V_{Tot}, $V_{S\text{-}Vol}/V_{Tot}$, V_{Refr}/V_{Tot}
Ny-Ålesund, Grubbenbade 75 m asl:					
Mar.–Apr. 1989	Aitken mode				
(Covert and Heintzenberg, 1993)	30 ($d_{Mode} = 48$ nm)				
	Accumulation mode				
	150 ($d_{Mode} = 220$ nm)				
Zeppelin station, 474 m asl:					
1979–1989[a], sum., wint.	145, 370 ($d > 5$ nm)		$1.5, 16.0 \times 10^{-6}$	5, 66	
Mar. 1990–Apr. 1992, sum., wint.	320, 172 ($d > 5$ nm)		$1.7, 5.7 \times 10^{-6}$	11, 93	
(Heintzenberg and Leck, 1994)					
Zeppelin station, 474 m asl:					
Feb.–May 1994	314 ($d > 5$ nm)		5.0×10^{-6}		
(Beine et al., 1996)	117 ($d > 10$ nm)				
Zeppelin station, 474 m asl:					
Apr.–May 1996	220 ($d > 10$ nm)	33 ($d > 10$ nm)			
(Staebler et al., 1999)					
Zeppelin station, 474 m asl:					
Aug.–Sept. 1998 (LSF I)	80 ($d = 15$–720 nm)	33 ($d > 10$ nm)		18	0.49, 0.33, 0.18
Apr.–May 1999 (LSF II)	–	–		71	
(this study)					
Ny-Ålesund, Amundsen mast:[a]					
Feb.–Mar., 2001 (NICE Dark)	275 ($d = 14$–740 nm)	39 ($d > 14$ nm)	5.76×10^{-6}	72	0.39, 0.22, 0.39
Apr.–May, 2001 (NICE Light)	860 ($d = 14$–740 nm)	80 ($d > 14$ nm)	7.80×10^{-6}	41	0.50, 0.27, 0.22
(this study)					

asl, above sea level; sum., summer; wint., winter.

[a]Measurements at sea level.

Heintzenberg, 1993; Heintzenberg and Leck, 1994; Beine et al., 1996; Staebler et al., 1999), and may thus be compared with those from our LSF and NICE intensives in Table 2. Considering the different measurement periods and methods, results presented here are similar to previous studies. An important aspect to consider in this comparison is the difference in site altitude between Ny-Ålesund and Zeppelin station. A recent sodar study during the spring and summer indicated that prevailing winds are predominantly southeasterlies at Ny-Ålesund and southerlies at Zeppelin station (Beine et al., 2001b). Wind conditions are mainly governed by orographic steering of the large-scale wind fields with katabatic winds transporting cold dense air from inland glaciers to the warmer Kongsfjorden Fjord. At other times, the open sea towards the west influences Ny-Ålesund with Arctic marine boundary layer (MBL) air masses. The relative influence of boundary layer versus free tropospheric conditions at Zeppelin station remains to be better characterized. However, web camera observations of the cloud top indicate that boundary layer conditions may be quite frequent (Ström et al., 2003). A comparison of the aerosol scattering coefficient ($\lambda = 550$ nm) at Zeppelin and at the NICE site revealed a ratio of 0.34 and $\sim$0.87 for February to May 2001. Part of the difference may be explained both by the use of a submicrometre cyclone inlet and the higher frequency of in-cloud events at Zeppelin which would result in lower σ_{SP} values. However, this cannot explain the full difference. Higher values at the NICE site imply a higher accumulation mode concentration, as well as a certain decoupling of the surface layer and the free troposphere. For instance, it is known that the Japanese station at Ny-Ålesund Rabben Airport (sea level) is more influenced by sea spray than Zeppelin station. Nevertheless, the high correlation suggests that measurements are similar at both sites when considering synoptic-scale air masses. Although our dataset is limited to a 3-month period it agrees well with an observed winter maximum and summer minimum in various aerosol physical and chemical parameters at the former Ny-Ålesund station at Gruvebadet (sea level; Maenhaut et al. 1989) and at Zeppelin station (Heintzenberg and Leck, 1994; Ström et al., 2003; K. Eleftheriadis, unpublished data). A similar cycle in aerosol concentration occurs at other Arctic sites, such as Barrow, Alaska (Polissar et al., 2001) and Alert, Canada (Sirois and Barrie, 1999), and is considered to be largely due to the seasonal position of the Arctic polar vortex. The encircling belt of cyclones which accompany the vortex lies southward of major pollution sources in Northern Eurasia

during the summer and northward in winter, resulting in Arctic haze events. The observed annual cycle at sites in the high Arctic contrasts a summer maximum and winter minimum at mid-latitude European sites, such as in Scandinavia (Tunved et al., 2003) or the Swiss Alps (Nyeki et al., 1998).

3.2. *Volatile aerosol properties: time-series and spectra*

Before discussing aerosol volatility results, it would be useful to establish to what extent the aerosol volatile and semi-volatile volumes (V_{Vol} and $V_{\text{S-Vol}}$) correspond to H_2SO_4 and bisulfate/sulfate species. Smith and O'Dowd (1996) used the volatility technique during ship campaigns in the North Sea and North Atlantic Ocean, and were able to qualitatively distinguish H_2SO_4 and bisulfate/sulfate components. In a similar manner, Fig. 3 shows a typical thermograph of aerosol volume as a function of volatility temperature for A and A& RA air masses during the Dark intensive. Similar thermographs were also found during the Light intensive. Despite the coarse temperature resolution, it can be seen that a large fraction (0.3–0.4) of the aerosol volatile volume was removed up to $T = 95\ ^\circ$C, while further heating to $T = 130\ ^\circ$C removed a much smaller fraction (<0.09). Similarly, a large decrease (0.15–0.2) was observed between $T = 130$ and 200 °C, followed by a small decrease (∼0.05) thereafter up to 300 °C. Laboratory calibration of the thermodenuder with H_2SO_4 and $(NH_4)_2SO_4$ aerosols determined that $95 \pm 3\%$ of the aerosol volume was removed at $T = 130$ and 225 °C, respectively. This suggests that H_2SO_4 and bisulfate/sulfate were major components of ambient aerosols, which is also confirmed by aerosol chemical speciation of impactor samples (Teinilä et al., 2003).

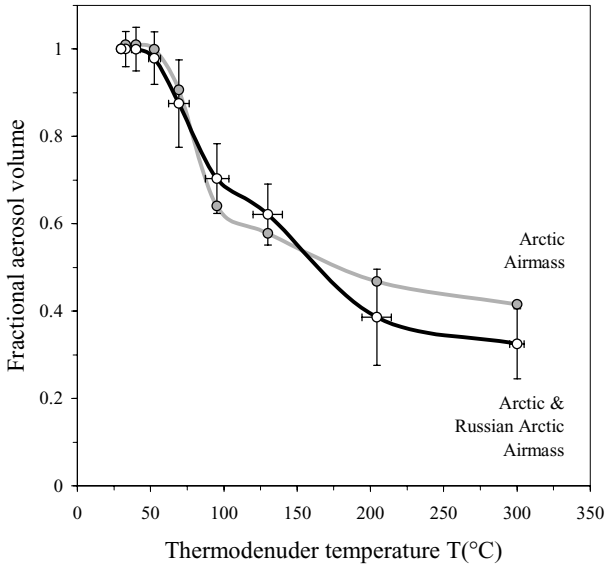

Fig 3. Thermograph of the fractional aerosol volume for two different air masses during the Dark intensive. Measurement uncertainty bars indicate ±1 standard deviation.

Nevertheless, the presence of OC compounds is not ruled out, and hence the aerosol volume removed at $T = 130$ and 300 °C will continue to be referred to here as V_{Vol} and $V_{\text{S-Vol}}$.

As we were also interested in the temporal behaviour of the aerosol mass concentration during NICE, time-series of fractional aerosol volumes ($V_{\text{Vol}}/V_{\text{Tot}}$, $V_{\text{S-Vol}}/V_{\text{Tot}}$ and $V_{\text{Rer}}/V_{\text{Tot}}$) are illustrated in Figs 1c and 2c. Due to the variability in 1 h and 12 h averages, 7 d running means are also included for illustrative purposes. The trend in the volatile fraction during the Dark intensive was largely invariant with $V_{\text{Vol}}/V_{\text{Tot}} \sim 0.40$, while an increase in the semi-volatile fraction from $V_{\text{S-Vol}}/V_{\text{Tot}} \sim 0.20$ to ∼0.35 meant a corresponding decrease in the refractory fraction from $V_{\text{Refr}}/V_{\text{Tot}} \sim 0.4$ to ∼0.25 (i.e. $V_{\text{Vol}}/V_{\text{Tot}} + V_{\text{S-Vol}}/V_{\text{Tot}} + V_{\text{Refr}}/V_{\text{Tot}} = 1$). The high acidity of the bulk aerosol from impactor measurements is also confirmed by the charge equivalent (CE) ratio of NH_4^+ and non-sea-salt (nss) SO_4^{2-} concentrations which was in the range 0.3–0.4 (Teinilä et al., 2003). The intrusion of anthropogenic air masses is evident when BC is elevated. These events usually coincided with an increase in $V_{\text{Refr}}/V_{\text{Tot}}$ (e.g. ∼ DOY 71 and 76) but this was not always the case (e.g. ∼ DOY 63.5 and 66). The most likely reason is that air masses with elevated $V_{\text{Refr}}/V_{\text{Tot}}$ were observed to come from Central Russia/Siberia where anthropogenic sources would be responsible for elevated BC concentrations. Air masses without elevated $V_{\text{Refr}}/V_{\text{Tot}}$ values were observed to come from the Arctic or Russian Arctic regions. Trajectory analysis indicated a residence time longer than 5 d in these regions during which aerosol coagulation and condensation of sulfate species etc would explain the lower than expected $V_{\text{Refr}}/V_{\text{Tot}}$ values.

Aerosol thermodenuder measurements at the beginning of the Light intensive were similar to those during the latter part of the Dark intensive, with $V_{\text{Vol}}/V_{\text{Tot}} \sim 0.40$, $V_{\text{S-Vol}}/V_{\text{Tot}} \sim 0.35$, $V_{\text{Refr}}/V_{\text{Tot}} \sim 0.25$. Towards the end of the Light intensive, the increase in aerosol concentrations during the two haze events discussed earlier was accompanied by a significant increase in $V_{\text{Vol}}/V_{\text{Tot}}$ to ∼0.85 which then returned to former levels. Corresponding NH_4^+/nss-SO_4^{2-} CE ratios were <0.1 indicated a strongly acidic aerosol (Teinilä et al., 2003). In addition, annular denuders gave peak concentrations of 4.4 μg m^{-3} for SO_2 and 4.3 μg m^{-3} for submicrometre SO_4^{2-} (Beine et al., 2003). A similar haze event with low NH_4^+/nss-SO_4^{2-} CE ratios was measured by Staebler et al. (1999). The air mass was relatively clean, without an enhanced accumulation-mode concentration, and originated from Greenland (5 d back-trajectory).

Figure 2 shows that the volatile component of the aerosol during both haze events lies almost exclusively in the accumulation mode (see also later discussion of Figs 4c and 5c). Nucleation events probably occurred earlier in the air mass history, and ageing through aerosol coagulation and condensation would then be responsible for the relatively large d_G (number geometric mean diameter) at 181 nm of the accumulation mode. Despite elevated SO_2 concentrations, the large values of S would then have prevented further nucleation from occurring. It is interesting to note

that towards the end of each haze event, $V_{\text{S-Vol}}/V_{\text{Tot}}$ increases from ~0.1 (see Fig. 2c, ~ DOY 126–128 and DOY 133–134) to previous levels of ~0.4–0.5. An explanation in terms of the conversion of H_2SO_4 to ammonium bisulfate/sulfate is feasible but it may simply be due to mixing and dilution with other air masses. The origin of these air masses is, however, not quite so straightforward to ascertain. Five-day back-trajectories indicated an origin from Central Russia/Siberia, but the BC concentration (range = 40–80 ng m^{-3}; average = 54 ng m^{-3}) is quite low and comparable to concentrations in earlier Arctic air masses (DOY 96 to 114, Fig. 2a). In addition, a study of the ^{210}Pb cycle during 2001 at Zeppelin indicated elevated concentrations during this period (Paatero et al., 2003). Continents are the predominant source of ^{210}Pb, although elevated concentrations are also observed during Arctic haze events when aerosol wet and dry deposition are minimal.

Due to the high sulfate concentrations observed during both haze events, natural as well as anthropogenic sources may be responsible. For instance, methanesulfonate (MSA), a tracer of biogenic sulfur emissions from oceanic dimethyl sulfide (DMS), exhibited concentrations less than the detection limit and ~50 ng m^{-3} during the Dark and Light intensives (excluding haze events), respectively (Teinilä et al., 2003). This corresponds to a MSA/nss-SO_4 ratio of ~9% during the latter, and compares with 28% measured by Heintzenberg and Leck (1994) in a summer campaign at Ny-Ålesund. In contrast, MSA was only elevated during the second haze event when a maximum of 130 ng m^{-3} was observed (MSA/nss-SO_4 ~ 2%), and indicates a small contribution from biogenic sources. On the other hand, Ström et al. (2003) suggested that the Siberian Arctic tundra could also serve as a potential source of aerosol precursor gases during thawing in spring/summer. However, anthropogenic emissions from central Russia/Siberia are probably of greater importance, where several industrial regions lie within the springtime polar front. A trajectory study by Vinogradova (2000) suggested that apart from Northern Europe and the Kola Peninsula, the Pechora Basin and Norilsk regions were important sources of heavy metal atmospheric pollutants. Trajectories for both haze events passed over the latter two regions. Emissions of SO_2 and the subsequent conversion to SO_4^{2-} over frozen land and ocean surfaces, where NH_3 emissions are minimal, would then account for the high acidity of the aerosol. The low correlation of BC with S and σ_{SP} is still difficult to fully explain but may have resulted from mixing of natural and anthropogenic air masses.

The decreasing trend in aerosol concentration and in $V_{\text{Refr}}/V_{\text{Tot}}$ occurs simultaneously to a decrease in BC concentration (Figs 1b, c and 2b, c). The high correlation coefficient $R = 0.94$ between V_{Refr} and BC during the Dark intensive indicates that BC is the dominant component of the refractory aerosol. However, this was not the case during the Light intensive where $R = 0.47$ for the whole period ($R = 0.35$ exclusive of both haze events; $R = 0.56$ during both haze events). These observations are explained if the sources, sinks and size ranges of the different refractory aerosol components are considered. Aged BC aerosols reside in the accumulation-mode size range and are primarily of anthropogenic origin in the Arctic due to long-range transport. However, as mineral dust and sea-salt aerosols reside in the coarse-mode size range ($d > 1$–2 μm) their sources are of a more local origin. As a result, the influence of mineral dust and sea salt is expected to be lower due to the snow/ice cover over land and sea during the winter but may increase as summer approaches. The above-discussed volume fractions from NICE are similar to average values of $V_{\text{Vol}}/V_{\text{Tot}} = 0.49$, $V_{\text{S-Vol}}/V_{\text{Tot}} = 0.33$ and $V_{\text{Refr}}/V_{\text{Tot}} = 0.18$ during the LSF I intensive in late summer 1998.

Examination of volatility spectra, averaged over specific air mass periods, also reveals further physical/chemical characteristics. Average N spectra during the Dark and Light intensives are shown in Fig. 4 which include log-normal parameters (N, d_{G} and σ_{G} (geometric standard deviation)) for ambient thermodenuder channels in each panel. The ambient size distribution for the Dark intensive in Fig. 4a illustrates a distinct accumulation but a less distinct Aitken mode ($d = 10$–100 nm). An increase in thermodenuder temperature results in a decrease in both N and d_{G}. Depending on the thermodenuder temperature an ideal sulfate/BC internal aerosol would exhibit a reduction in d_{G} but no change in N. In contrast, an ideal sulfate and BC external aerosol would exhibit a complete or significant decrease in N, and a possible change in d_{G} if both aerosol components had different initial values of d_{G}. Although the mixing state of the aerosol cannot be determined in this manner, the aerosol measured during the Dark intensive was most likely an aged aerosol which mixed with less-aged air masses *en route*. The first part of the Light intensive was characterized by low aerosol concentrations in Russian Arctic and Western European air masses. VSMPS spectra in Fig. 4b, excluding the above-mentioned haze events, were also similar with the exception of a distinct Aitken mode ($N = 268$ cm^{-3}; $d_{\text{G}} = 31$ nm) at ambient conditions, and disappeared upon heating to $T = 130$ °C. These Aitken aerosols were most probably H_2SO_4 and formed by nucleation up to 24–36 h previously. These observations of number size distribution agree well with a 12-month study of aerosol size spectra at Zeppelin from March 2000 to March 2001, for which $d_{\text{G}} \sim 40$ and 150 nm were observed for the Aitken and accumulation modes, respectively (Ström et al., 2003). A further interesting feature frequently observed was a nucleation mode ($d < 10$–20 nm). Part of the mode is discernible for average (Fig. 4b) as well as median values (not shown), and most probably resulted from nucleation several hours previously. Similar observations of new particle formation in the Arctic during spring have been made in previous studies. Nilsson et al. (2001) found that nucleation at rural sites in Finland was enhanced in spring and autumn which generally coincided with the intrusion of Arctic and polar air masses. The composition of new particles has been mainly attributed to nucleation of H_2SO_4 (Covert and Heintzenberg, 1993;

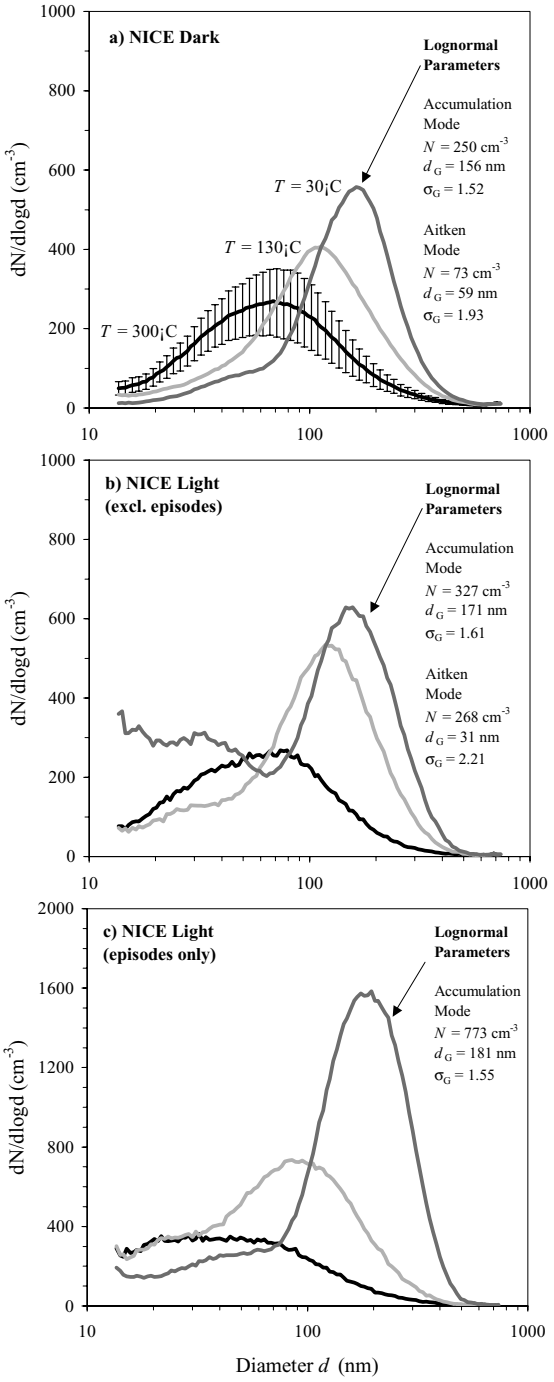

Fig 4. Aerosol number size (N) spectra at thermodenuder temperatures $T = 25$, 130 and 300 °C (dark grey, light grey and black curves respectively) averaged over the periods: (a) Dark intensive, DOY = 52–67 and (b) Light intensive, DOY = 114–123.9 and 136.1–139, i.e. excluding both haze events, and (c) Light intensive, DOY = 123.9–136.1, i.e. haze events only. Note the absence of Aitken-mode log-normal parameters (ill-posed fit) and the difference in the scales of parts a and b and part c by a factor of 2. Measurement uncertainty bars (±1 standard deviation) are only shown for $T = 300$ °C in panel a for clarity.

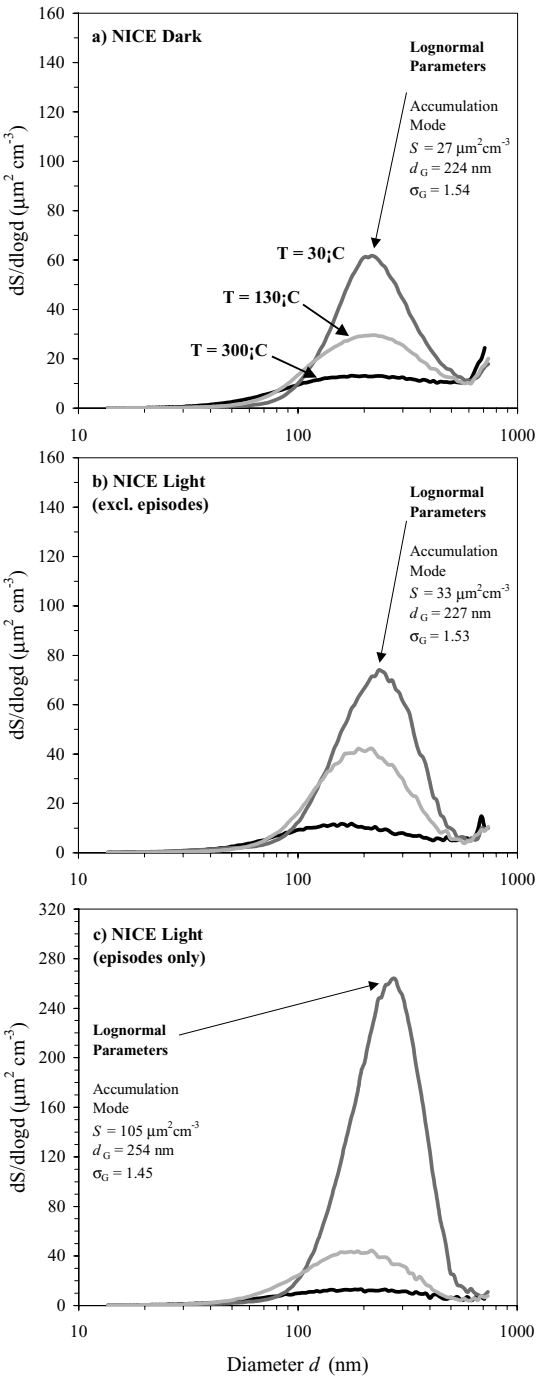

Fig 5. Same as for Fig. 4, except for aerosol surface area (S) spectra. Note that the scales in parts a and b and part c differ by a factor 2.

Wiedensohler et al., 1996) as well as OC aerosols (Leck and Bigg, 1999). The role of OC aerosols at remote locations is beginning to be more widely studied. In a recent study Narukawa et al. (2002) found that dicarboxylic acids were the largest constituent of Arctic organic aerosols. Enhanced concentrations of oxalic (C_2), malonic (C_3) and succinic (C_4) acids during the

Arctic spring were attributed to photochemical oxidation of organic pollutants, residing in the Arctic during winter. In contrast to the nucleation events in Fig. 4b, spectra of haze events during the Light intensive in Fig. 4c exhibit the distinct absence of an Aitken mode as well as an enhanced accumulation-mode concentration ($N = 773$ cm^{-3}). A number geometric mean diameter at 181 nm is close to that observed for Arctic haze ($d_G \sim 200$ nm) in a previous study at Zeppelin station (Covert and Heintzenberg, 1993). These facts further suggest that air masses during the Light intensive were of well-aged, continental origin.

Figures 5a–c show S spectra for the corresponding periods in Figs 4a–c and illustrate the dominance of a monomodal accumulation mode at $d_G = 220$–230 nm which agrees well with $d_G \sim 200$ nm for springtime measurements at Zeppelin by Ström et al. (2003). These investigators found that aerosol surface area and volume concentrations in spring were up to six times higher than during other seasons, which was attributed to Arctic haze events. Returning to Figs 4a–c, spectra for the aerosol volume were similar in shape (not shown). A volume mean geometric diameter at ∼300 nm was found which corresponds well with the mass mean geometric diameter for NH_4^+ and SO_4^{2-} species at 310 nm from impactor measurements (Teinilä et al., 2003). It should be noted that our measurements are for dried aerosols at RH ∼10%, and are similar to those of Staebler et al. (1999) who used an optical particle counter (at RH ∼ 5%) at Zeppelin in the spring of 1996. In their study, aerosol spectra were corrected for ambient RH (78–90%) using an aerosol hydration growth model. It was found that S and V in the accumulation mode increased by factors of 3 and 5, respectively, corresponding to an average increase in the surface and volume mean diameter by 60–80%. No such correction was made to the present data set, but it illustrates to what extent ambient S and V concentrations may differ from those measured, and to what extent this must be accounted for in aerosol physical models.

4. Conclusions

In summary, aerosol measurements conducted at Ny-Ålesund before and after Arctic sunrise in 2001 during the NICE campaign were dominated by Arctic and sub-Arctic air masses. These were characterized by low number ($N \sim 275$ and 590 cm^{-3} respectively) and surface area ($S \sim 39$ and 28 μm^2 cm^{-3}) concentrations (measured range $d = 14$–740 nm) except for two haze events with high concentrations in springtime ($N \sim 1140$ cm^{-3} and $S \sim 125$ μm^2 cm^{-3}). Excluding these haze events, aerosol volatility measurements indicated no significant variation in the volatile (∼0.40), semi-volatile (∼0.32) or refractory (∼0.28) volume fractions which are generally attributed to H_2SO_4, $(NH_4)_2SO_4/NH_4HSO_4$ and soot/dust/sea-salt aerosol. An in-depth case study of aerosol properties with respect to renoxification will be given in a follow-on paper.

5. Acknowledgments

We thank Kim Holmén for data from the Zeppelin station. Funding from the European Union LSF and 5th Framework (contract no EVK2-1999-00029) programmes is kindly acknowledged.

References

Aumont, B., Madronich, S., Ammann, M., Baltensperger, U. and Hauglustaine, D. 1999. On the NO_2 + soot reaction in the atmosphere. *J. Geophys. Res.* **104**, 1729–1736.

Beine, H. J., Engardt, M., Jaffe, D. A., Hov, Ø., Holmén, K. et al. 1996. Measurements of NO_x and aerosol particles at the Ny Ålesund Zeppelin mountain station on Svalbard: influence of regional and local pollution sources. *Atmos. Environ.* **30**, 1067–1079.

Beine, H. J., Allegrini, I., Sparapani, R., Ianniello, A. and Valentini, F. 2001a. Three years of springtime trace gas and particle measurement at Ny-Ålesund, Svalbard. *Atmos. Environ.* **35**, 3645–3658.

Beine, H. J., Argentini, S., Maurizi, A., Mastrantonio, G. and Viola, A. 2001b. The local wind field at Ny-Ålesund and the Zeppelin mountain at Svalbard. *Meteorol. Atmos. Phys.* **78**, 107–113.

Beine, H. J., Dominé, F., Ianniello, A., Nardino, M., Allegrini, I. et al. 2003. Fluxes of nitrates between snow surfaces and the atmosphere in the European high Arctic. *Atmos. Chem. Phys.* **3**, 335–346.

Burtscher, H., Baltensperger, U., Bukowiecki, N., Cohn, P., Hüglin, C. et al. 2001. Separation of volatile and non-volatile aerosol fractions by thermodesorption: instrumental development and applications. *J. Aerosol Sci.* **32**, 427–442.

Cecinato, A., Mabilia, R. and Marino, F. 2000. Relevant organic compounds in ambient particulate matter collected at Svalbard Islands (Norway). *Atmos. Environ.* **34**, 5061–5066.

Covert, D. S. and Heintzenberg, J. 1993. Size distributions and chemical properties of aerosol at Ny Ålesund, Svalbard. *Atmos. Environ.* **27A**, 2989–2997.

Dibb, J. E., Arsenault, M., Peterson, M. C. and Honrath R. E. 2002. Fast nitrogen oxide photochemistry in Summit, Greenland snow. *Atmos. Environ.* **36**, 2501–2511.

Draxler, R. R. and Hess, G. D. 1998. An overview of the HYSPLIT4 modelling system for trajectories, dispersion and deposition. *Aust. Meterorol. Mag.* **79**, 295–308.

Hauglustaine, D. A., Ridley, B. A., Solomon, S., Hess, P. G. and Madronich, S. 1996. HNO_3/NO_x ratio in the remote troposphere during MLOPEX2: evidence for nitric acid reduction on carbonaceous aerosols? *Geophys. Res. Lett.* **23**, 2609–2612.

Heintzenberg, J. and Leck, C. 1994. Seasonal variation of the atmospheric aerosol near the top of the marine boundary layer over Spitsbergen related to the Arctic sulphur cycle. *Tellus* **46B**, 52–67.

Honrath, R. E., Peterson, M. C., Dziobak, M. P., Green, S. and Dibb, J. E. 2000. Release of NO_x from sunlight-irradiated midlatitude snow. *Geophys. Res. Lett.* **27**, 2237–2240.

Leck, C. and Bigg, E. K. 1999. Aerosol production over remote marine areas—a new route. *Geophys. Res. Lett.* **26**, 3577, 3580.

Maenhaut, W., Cornille, P., Pacyna, J. M. and Vitols, V. 1989. Trace element composition and origin of the atmospheric aerosol in the Norwegian Arctic. *Atmos. Environ.* **23**, 2551–2569.

Narukawa, M., Kawamura, K., Li, S.-M. and Bottenheim, J. W. 2002. Dicarboxylic acids in the Arctic aerosols and snowpacks collected during ALERT 2000. *Atmos. Environ.* **36**, 2491–2499.

Nilsson, E. D. and Barr, S. 2001. Effects of synoptic patterns on atmospheric chemistry and aerosols during the Arctic Ocean Expedition 1996. *J. Geophys. Res.* **106**, 32 069–32 086.

Nilsson, E. D., Paatero, J. and Boy, M. 2001. Effects of air masses and synoptic weather on aerosol formation in the continental boundary layer. *Tellus* **53B**, 462–478.

Nyeki, S., Li, F., Weingartner, E., Streit, N., Colbeck, I., Gäggeler, H. W. et al. 1998. The background aerosol size distribution in the free troposphere: an analysis of the annual cycle at a high-alpine site. *J. Geophys. Res.* **103**, 31 749–31 761.

Paatero, J., Hatakka, J., Holmén, K., Eneroth, K. and Viisanen, Y. 2003. Lead-210 concentration in the air at Mt. Zeppelin, Ny-Ålesund, Svalbard. *Phys. Chem. Earth* **28**, 1175–1180.

Polissar, A. V., Hopke, P. K. and Harris, J. M. 2001. Source regions for atmospheric aerosol measured at Barrow, Alaska. *Environ. Sci. Technol.* **35**, 4214–4226.

Sirois, A. and Barrie, L. A. 1999. Arctic lower tropospheric aerosol trends and composition at Alert, Canada: 1980–1995. *J. Geophys. Res.* **104**, 11599–11618.

Smith, M. H. and O'Dowd, C. D. 1996. Observations of accumulation mode aerosol composition and soot carbon concentrations by means of a high-temperature volatility technique. *J. Geophys. Res.* **101**, 19 583–19 591.

Staebler, R., Toom-Sauntry, D., Barrie, L., Langendörfer, U., Lehrer, E. et al. 1999. Physical and chemical characteristics of aerosols at Spitsbergen in the spring of 1996. *J. Geophys. Res.* **104**, 5515–5529.

Ström, J., Umegård, J., Tørseth, K., Tunved, P., Hanson, H.-C. et al. 2003. One year of particle size distribution and aerosol chemical composition measurements at the Zeppelin Station, Svalbard, March 2000–March 2001. *Phys. Chem. Earth* **28**, 1181–1190.

Svendsen, H., Beszczynska-Møller, A., Hagen, J. O., Lefauconnier, B., Tverberg, V. et al. 2002. The physical environment of Kongsfjorden-Krossfjorden, an Arctic fjord system in Svalbard. *Polar Res.* **21**, 133–166.

Teinilä, K., Hillamo, R., Kerminen, V.-M. and Beine, H. J. 2003. Aerosol chemistry during the NICE dark and light campaigns. *Atmos. Environ.* **37**, 563–575.

Tunved, P., Hansson, H.-C., Kulmala, M., Aalto P., Viisanen, Y., Karlsson, H. et al. 2003. One year boundary layer aerosol size distribution data from five Nordic background stations. *Atmos. Chem. Phys.* **3**, 2183–2205.

Vinogradova, A. A. 2000. Anthropogenic pollutants in the Russian Arctic atmosphere: sources and sinks in spring and summer. *Atmos. Environ.* **34**, 5151–5160.

Wiedensohler, A., Covert, D. S., Swietlicki, E., Aalto, P., Heintzenberg, J. et al. 1996. Occurrence of an ultrafine particle mode less than 20 nm in diameter in the marine boundary layer during Arctic summer and autumn. *Tellus* **48B**, 213–222.